Hearing Research 302 (2013) 84–95

Contents lists available at SciVerse ScienceDirect

Hearing Research

journal homepage: www.elsevier.com/locate/heares

Research paper

Cochlear implant artifact attenuation in late auditory evoked potentials: A single channel approach

Myles Mc Laughlin [a,b,*], Alejandro Lopez Valdes [b], Richard B. Reilly [b], Fan-Gang Zeng [a]

[a] Hearing and Speech Laboratory, University of California Irvine, USA
[b] Neural Engineering Group, Trinity College Dublin, Ireland

ARTICLE INFO

Article history:
Received 10 December 2012
Received in revised form
7 May 2013
Accepted 12 May 2013
Available online 28 May 2013

ABSTRACT

Recent evidence suggests that late auditory evoked potentials (LAEP) provide a useful objective metric of performance in cochlear implant (CI) subjects. However, the CI produces a large electrical artifact that contaminates LAEP recordings and confounds their interpretation. Independent component analysis (ICA) has been used in combination with multi-channel recordings to effectively remove the artifact. The applicability of the ICA approach is limited when only single channel data are needed or available, as is often the case in both clinical and research settings. Here we developed a single-channel, high sample rate (125 kHz), and high bandwidth (0–100 kHz) acquisition system to reduce the CI stimulation artifact. We identified two different artifacts in the recording: 1) a high frequency artifact reflecting the stimulation pulse rate, and 2) a direct current (DC, or pedestal) artifact that showed a non-linear time varying relationship to pulse amplitude. This relationship was well described by a bivariate polynomial. The high frequency artifact was completely attenuated by a 35 Hz low-pass filter for all subjects ($n = 22$). The DC artifact could be caused by an impedance mismatch. For 27% of subjects tested, no DC artifact was observed when electrode impedances were balanced to within 1 kΩ. For the remaining 73% of subjects, the pulse amplitude was used to estimate and then attenuate the DC artifact. Where measurements of pulse amplitude were not available (as with standard low sample rate systems), the DC artifact could be estimated from the stimulus envelope. The present artifact removal approach allows accurate measurement of LAEPs from CI subjects from single channel recordings, increasing their feasibility and utility as an accessible objective measure of CI function.

© 2013 Elsevier B.V. All rights reserved.

1. Introduction

Advances in cochlear implant (CI) technology now mean that a typical recipient of a modern CI can expect to understand speech in a quiet listening environment (for a review see Zeng et al., 2008). In spite of these advances there remains a large amount of variability in performance across users. Behavioral methods such as speech perception tests or non-speech based listening tests (Fu, 2002; Henry and Turner, 2003; Henry et al., 2005; Won et al., 2007) can be used to quantify this variability. However, behavioral methods are often not suitable for pediatric CI users and speech-based tests may not be the best way to assess the performance of new CI recipients while they are still learning to understand speech heard through their implants. Neural based objective metrics of performance may provide a useful alternative to behavioral testing for both these user groups. In addition to potentially improving the standard of treatment received by an individual CI user, the development of neural objective metrics of CI performance may also advance our understanding of the origins of the performance variability, by giving information on the underlying neural mechanisms. However, the development of such neural metrics has been hampered by the large CI related electrical artifact, which contaminates evoked potential recordings in these subjects.

Firszt et al. (2002) found that cortical evoked potentials may be useful for predicting speech perception outcomes for CI. However, to minimize the artifact, this study used very short simple stimuli which are unable to fully probe the complex processing that takes place in the auditory system. Gilley et al. (2006) proposed a method for attenuating the artifact caused by longer duration stimuli. They showed how independent component analysis (ICA) could be used to recover late auditory evoked potentials (LAEP) from multi-channel data. Utilizing the multi-channel ICA approach, two recent studies by Zhang et al. (2010, 2011) showed how LAEPs

* Corresponding author. 110 Medical Sciences E, University of California Irvine, Irvine, CA 92697, USA. Tel.: +1 949 282 7667.
E-mail address: myles.mclaughlin@uci.edu (M. Mc Laughlin).

0378-5955/$ – see front matter © 2013 Elsevier B.V. All rights reserved.
http://dx.doi.org/10.1016/j.heares.2013.05.006

obtained using a mismatch negativity paradigm can provide useful information on CI functionality and that this information can be related to behavioral outcomes such as speech perception. One drawback of the ICA approach is that multi-channel data must be acquired, even when, as with the two studies by Zhang et al., most of the results and conclusions are based on artifact-free single-channel data. Having to acquire multi-channel data necessitates the purchase of expensive multi-channel acquisition systems, increases subject preparation time, as a full EEG cap must be attached and, for CI subjects, adds to the difficulty of positioning the EEG cap over the behind-the-ear processor and magnetic link. For most clinical applications and many research questions, single-channel data are sufficient and subject preparation time much shorter. These practical considerations limit the applicability of the ICA-based artifact attenuation approach and led us to develop a single-channel based artifact attenuation approach.

To better understand the origin of the CI related artifact in LAEPs we developed a high-sample-rate, high-bandwidth, single-channel acquisition system with a temporal resolution high enough to clearly resolve each stimulation pulse. Here, we used this acquisition system to show that LAEPs recorded from CI subjects are generally composed of three components: a neural response component and two artifact components. Based on this signal composition, we proposed a three-stage artifact attenuation strategy (Fig. 1). The high frequency artifact (HFA) was found to be a direct representation of the stimulation pulses and was completely attenuated by a low-pass filter (stage 1). The low frequency or DC artifact (DCA), often referred to as a 'pedestal' artifact, could be accentuated by an electrode impedance mismatch and in some subjects could be attenuated by balancing the impedance of the recording electrodes (stage 2). Based on the assumption that the DCA was caused by the stimulation pulses, we developed a mathematical framework to obtain an estimate of the DCA and remove it from the LAEP (stage 3). Finally, we demonstrated how this single-channel approach could be also be applied with low sample rate data (commercial systems) and that it could be used to measure N1–P1 amplitude growth functions for CI users.

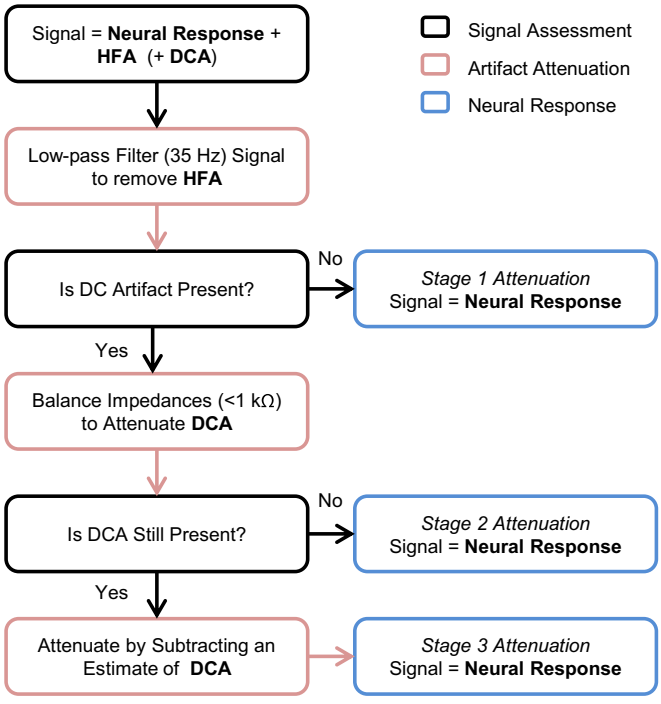

Fig. 1. Flow chart showing three stage artifact attenuation approach. The acquired signal (SIG) consisted of the neural response (NR) and two artifact components: a high frequency artifact (HFA) and a low frequency or DC artifact (DCA). A low-pass filter attenuated the HFA (stage 1). Balancing electrode impedances to within 1 kΩ attenuated the DCA for some subjects (stage 2). For the remaining subjects, the DCA could be estimated from the pulse amplitude or stimulus envelope and subtracted from the signal to leave the neural response (stage 3).

2. Material and methods

2.1. Subjects

LAEPs were measured for 22 adult CI subjects (7 male, 15 female) at two separate locations: Hearing and Speech Laboratory, University of California Irvine ($n = 7$) and Trinity Centre for Bioengineering, Trinity College Dublin ($n = 15$). Experimental procedures were approved by The University of California Irvine's Institutional Review Board and the Ethical Review Board at Trinity College Dublin. Informed consent was obtained from all subjects. Subjects were aged between 20 and 79 (mean 55, standard deviation 17) years and used a device from one of the three main manufacture's (Cochlear $n = 20$, Advanced Bionics $n = 1$, Med-El $n = 1$). All devices used monopolar stimulation strategies.

2.2. Stimuli

Stimuli consisted of tone bursts with frequencies of 250, 500 or 1000 Hz with durations of 100, 300 or 500 ms. Broadband noise stimuli (100–8000 Hz) were also used. Stimuli were presented at most comfortable level (MCL) and, when amplitude growth functions were collected, levels were decreased in equal decibel steps between MCL and threshold. Stimuli were generated in Matlab (Mathworks, Natick, MA) at a sampling rate of 44.1 kHz and a 10 ms on and off cosine squared ramp was applied. In Trinity College Dublin stimuli were presented through a standard PC soundcard and in University of California Irvine stimuli were presented through a DA converter (NI-USB 6221, National Instruments, Austin, TX). All stimuli were presented to the audio line in on the subject's CI. To limit the effects of any unwanted background noise, the CI microphone volume and sensitivity were set to the minimum allowable values. At University of California Irvine subjects were seated in a sound booth and at Trinity Centre for Bioengineering subjects were seated in a quiet room. Subjects used their everyday speech processing strategy without any special adjustments other than changes to the microphone volume and sensitivity. This method of stimulation was chosen, as opposed to using a research interface to directly control the CI, because it represents a worst case scenario in terms of the CI artifact. It was reasoned that this would result in the development of a robust artifact attenuation approach that could be easily applied in different settings and with different modes of stimulation.

Stimuli were always presented monaurally through channel one on the PC sound card or DA converter. For all stimuli, a trigger pulse at stimulus onset was presented on channel two of the output device. This trigger pulse was used to synchronize stimulus presentation and LAEP recording.

2.3. Evoked potential recordings

A high temporal resolution EEG acquisition system was developed. It consisted of a high bandwidth, low noise, single-channel differential amplifier (SRS 560, Stanford Research Systems, Sunnyvale, CA) connected to a high sample rate AD converter (NI-USB 6221, National Instruments, Austin, TX). The sample rate on the AD converter was set to 125 kS/s, the low-pass filter on the amplifier was typically set to 100 kHz and the high-pass filter was set to either DC, 0.03 Hz or 1 Hz. The filter roll-offs were set to 12 dB/Oct

and the low-noise gain mode was selected. Usually, the gain on the amplifier was set to 2000. For most subjects at most stimulation levels this gain setting ensured that the amplifier did not saturate during stimulation. Occasionally, at the highest stimulation levels, the gain was reduced to 1000 to avoid amplifier saturation. To reduce 50/60 Hz mains noise the amplifier was disconnected from the mains and operated in battery mode. The dynamic range on the AD converter was set to ±10 V. Standard gold cup surface electrodes were used. An electrode placed at Cz was connected to the positive input on the amplifier. On the side opposite to the CI being tested, an electrode placed on the mastoid was connected to the negative input on the amplifier, and one placed on the collar bone was connected to the amplifier ground. This system was designed to allow the CI related artifact to be clearly sampled with only minimal distortion being caused by the acquisition system.

Channel one on the AD converter was connected to the output of the amplifier and channel two was connected to the stimulus trigger pulse mentioned in the previous section. Custom software written in Matlab processed the output of the AD converter. Detection of the trigger pulses in software allowed accurate synchronization of the stimulus presentation with the recorded signal. The software performed online averaging, filtering, and visualization of the LAEP and stored the raw data for offline analysis. Long epochs of 300 ms pre-stimulus to 800 ms post-stimulus were used. All digital filters mentioned below were applied to the long, averaged, epochs. The use of long epochs minimizes any possible filter edge effects. For plotting and display purposes a shorter epoch of 100 ms pre-stimulus to 500 ms post-stimulus was used.

2.4. Artifact attenuation

LAEPs recorded with the high sample rate system using CI subjects were compared with typical LAEPs recorded using normal hearing subjects. This comparison showed that the signal (SIG) recorded in CI subjects consisted of a neural response component (NR), similar to that observed for normal hearing subjects, in addition to two visually distinct artifact components, a high frequency artifact (HFA) and a low frequency artifact (DCA). Thus the recorded signal could be represented by the following equation, where t is time,

$$\mathrm{SIG}(t) = \mathrm{NR}(t) + \mathrm{HFA}(t) + \mathrm{DCA}(t) \quad (1)$$

Based on this signal composition we developed a three stage, single-channel, artifact attenuation approach. Each stage is explained in detail below and a block diagram outlining the approach is shown in Fig. 1.

2.4.1. Stage 1: low-pass filter

Single, unaveraged recordings of the response to one stimulus presentation showed that the HFA was a direct representation of the stimulation pulses (see Fig. 2A and D). The HFA was completely attenuated by a low-pass filter (Fig. 2C and F). The low-pass filter was implemented in the custom Matlab software as a 2nd order Butterworth filter with a cutoff frequency of 35 Hz and 12 dB/Oct slope. This filter was applied using a zero-phase forward and reverse digital filtering technique (filtfilt command, Matlab). The HFA could also be attenuated by setting the hardware low-pass filter on the amplifier to 30 Hz with a 12 dB/Oct slope.

2.4.2. Stage 2: impedance balancing

After removal of the HFA a DCA was observed in the LAEPs from some subjects (Fig. 3). For some subjects this DCA could be attenuated by ensuring that the electrode impedances were balanced to within 1 kΩ (Fig. 4). To do this, the high impedance electrode was first identified by comparison of the impedances measured between all combinations of the three electrodes. The high impedance electrode was then removed, the skin prepared again and the electrode replaced.

2.4.3. Stage 3: DCA estimation

For some subjects, the DCA could not be fully attenuated by the impedance balancing. For these subjects, a DCA estimation method

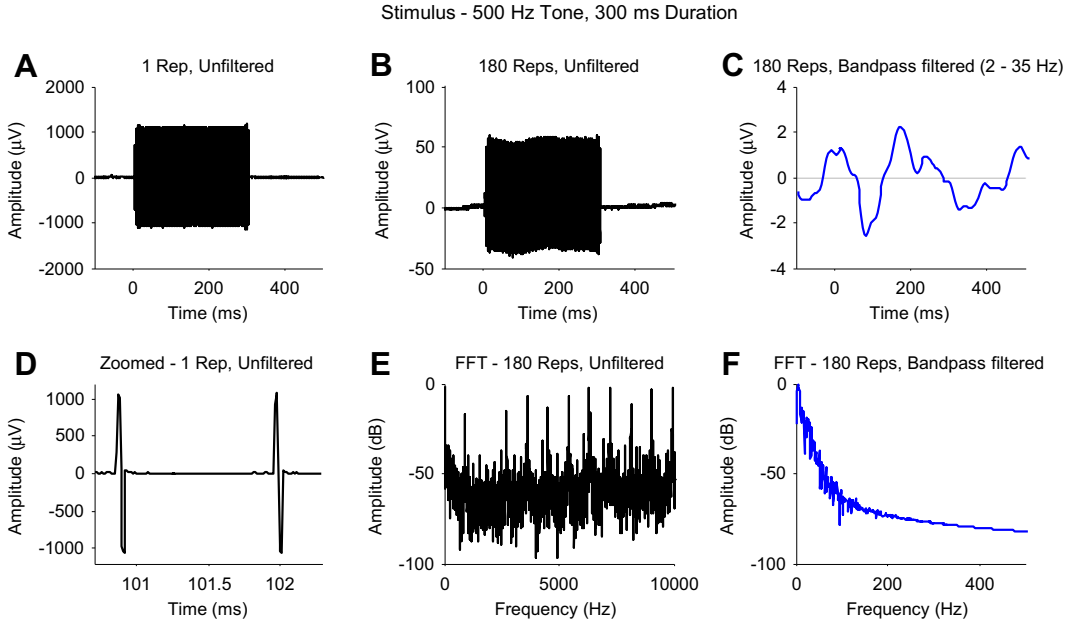

Fig. 2. A low-pass filter removed the high frequency artifact. A) The large amplitude high frequency artifact is clearly visible after only one repetition. B) As the individual stimulation pulses do not sum in phase the high frequency artifact becomes smaller with more repetitions. The low frequency envelope is caused by the neural response. C) A band-pass (2–35 Hz) filter attenuates the high frequency artifact to leave the neural response. D) Zooming in on one repetition shows the individual stimulation pulses. E) The frequency spectrum of the unfiltered average data shows the high frequency artifact at the stimulation rate and harmonics. F) The frequency spectrum of the filtered data shows the effect of the band-pass 2nd order Butterworth filter.

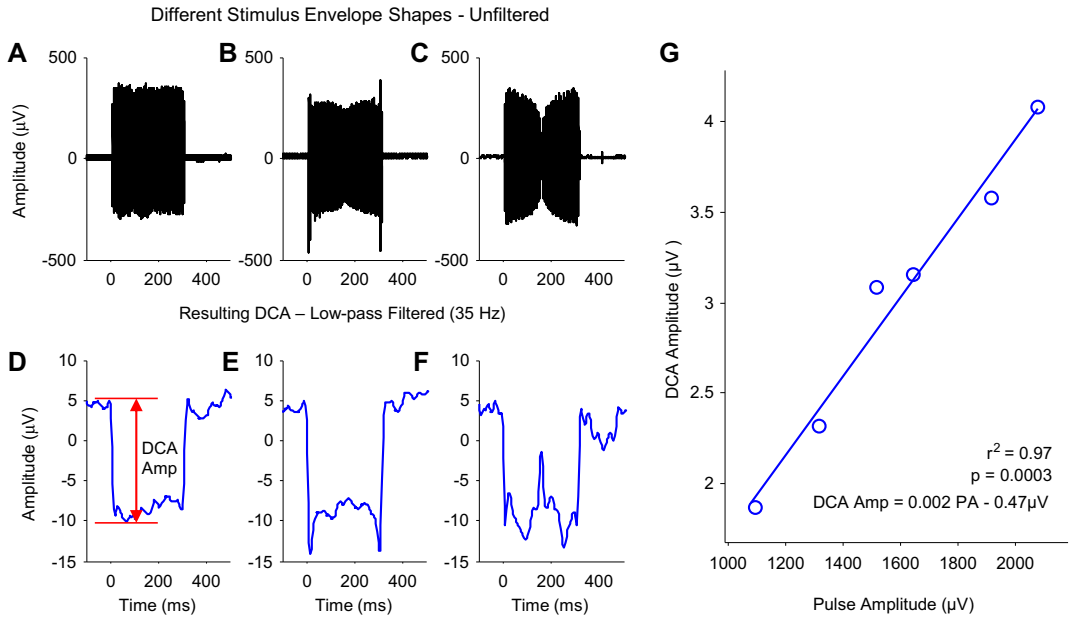

Fig. 3. DC artifact is related to pulse amplitude. A–B) The unfiltered averaged response from one subject to three stimuli with different envelope shapes. The pulse amplitude follows the stimulus envelope shape. E–F) The low-pass filtered data show a DC artifact which is related to the shape of the pulse amplitude. G) Data from a different subject showing a linear relationship between DC artifact amplitude and pulse amplitude.

was applied. Examination of the DCA showed that it was related to the stimulation pulses, i.e. the onset and offset times of the DCA were similar to those of both the HFA and the stimulus, and the shape of the DCA was similar to that of the acoustic stimulus envelope and the HFA envelope. Given these observations, it is reasonable to assume that the DCA can be described by a function of both stimulation pulse amplitude (PA) and time (t),

$$\mathrm{DCA} = f(\mathrm{PA}, t) \tag{2}$$

Examination of the DCA showed that this relationship was well approximated by a bivariate polynomial for all subjects,

$$\mathrm{DCA} = \sum_{ij} a_{ij} \mathrm{PA}^i t^j, \tag{3}$$

where a is a coefficient for each term in the polynomial and i and j determine the degree of the polynomial.

The CI stimulation pulse generator and stimulus onset are not synchronized. Therefore, pulses across repetitions are slightly jittered, with the result that the PA in the averaged signal is smaller than in a single repetition (compare Fig. 2A and B). To create a pulse-synchronized averaged signal, a cross correlation between the first repetition and all other repetitions was performed. The

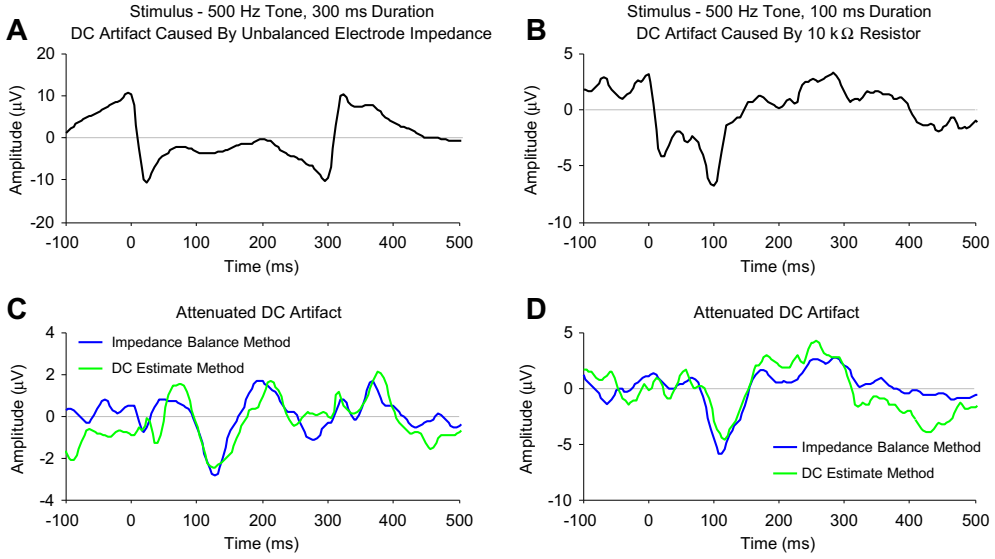

Fig. 4. The DC artifact can be caused by an impedance mismatch. A) A DC artifact was observed when the electrode impedances were unbalanced (Cz = 4.6, Mastoid = 2.9, Ground = 2.7 kΩ). B) Placing a 10 kΩ resistor between the Cz electrode and the amplifier also caused a DC artifact. C) Balancing the electrode impedances (Cz = 2.6, Mastoid = 2.6, Ground = 2.3 kΩ) attenuated the DC artifact (blue line). Applying the DC estimation method to the unbalanced data shown in panel A achieved a similar result (green line). D) Removing the resistor completely attenuated the DC artifact (blue line). Applying the DC estimation method to the unbalanced data shown in panel B A achieved a similar result (green line). (For interpretation of the references to colour in this figure legend, the reader is referred to the web version of this article.)

maximum time lag in the cross correlation was limited to one time period of the stimulation rate. This determined the amount of jitter between repetitions, which could then be applied as a small delay to each repetition to create a pulse-synchronized signal. An accurate measurement of PA could then be obtained from the pulse-synchronized signal.

Fig. 5 is a block diagram showing how the polynomial coefficients were estimated from the recorded signal to give an estimate of the DCA. Firstly, PA was measured from the unfiltered pulse-synchronized signal as a function of time. Next, the averaged (non-synchronized) signal was low-pass filtered to remove the HFA, leaving just the NR and DCA,

$$\mathrm{SIG_f}(t) = \mathrm{NR}(t) + \mathrm{DCA}(t) \quad (4)$$

The PA time series was filtered with a 2nd order digital Butterworth band-pass filter (compare the two upper right boxes on Fig. 5). The cut-off frequencies and slopes of this band-pass digital filter were matched to the cut-off frequencies and slopes of the filters applied to the signal: the high-pass setting used on the amplifier and low-pass used in the software for HFA attenuation. An estimate of the DCA was then obtained by fitting a bivariate polynomial to these data using the polyfitn function in Matlab (available for download from the Mathworks File Exchange). In the polynomial fitting function, the two independent variables were given as PA and t, and the dependent variable was $\mathrm{SIG_f}$. The parameters obtained from the fitting function, i.e. the coefficients a, could then be used in Eq. (3), together with the PA time series, to obtain an estimate of DCA ($\mathrm{DCA_{est}}$). To obtain the neural response, the DCA was attenuated by subtracting $\mathrm{DCA_{est}}$ from $\mathrm{SIG_f}$,

$$\mathrm{NR}(t) \approx \mathrm{SIG_f}(t) - \mathrm{DCA_{est}}(t) \quad (5)$$

To obtain a measure of PA, it is necessary to have high sample rate data, for which the stimulation pulses are clearly resolved. Most commercially available acquisition systems cannot acquire data at these high sample rates. When a measure of PA is not available, a measure of the stimulus envelope (SE) can be substituted. For vocoder-based speech processing strategies the SE will be related to the PA via a compression function.

2.4.3.1. Polynomial degree. We remind the reader that the degree (often referred to as order) of a polynomial is determined by the polynomial term with the largest degree, and that the degree of a polynomial term is determined by the sum of the exponents. Thus, a bivariate 3rd degree polynomial will contain PA^2t and $\mathrm{PA}t^2$ terms but not a PA^3t term. The degree of the polynomial which gave the best fit to that data was related to the number of non-linear transformations between the PA or SE and the recorded signal. The results section shows the effects of different acquisition system settings which influence these transformations and suggests the appropriate polynomial degree to be used in each case.

2.4.3.2. Constraining the fit. Eq. (3) shows the approximated relationship between DCA, PA and t. PA and t are known but the coefficients a and DCA are unknown. As described above, to estimate the coefficients a bivariate polynomial was fitted to PA, t and $\mathrm{SIG_f}$, where $\mathrm{SIG_f}$ contains both DCA and NR (see Eq. (4)). The most accurate estimate of DCA will be obtained when the fitting algorithm fits only the DCA component of $\mathrm{SIG_f}$ and not the NR component. A number of factors help constrain the fit to the DCA component only:

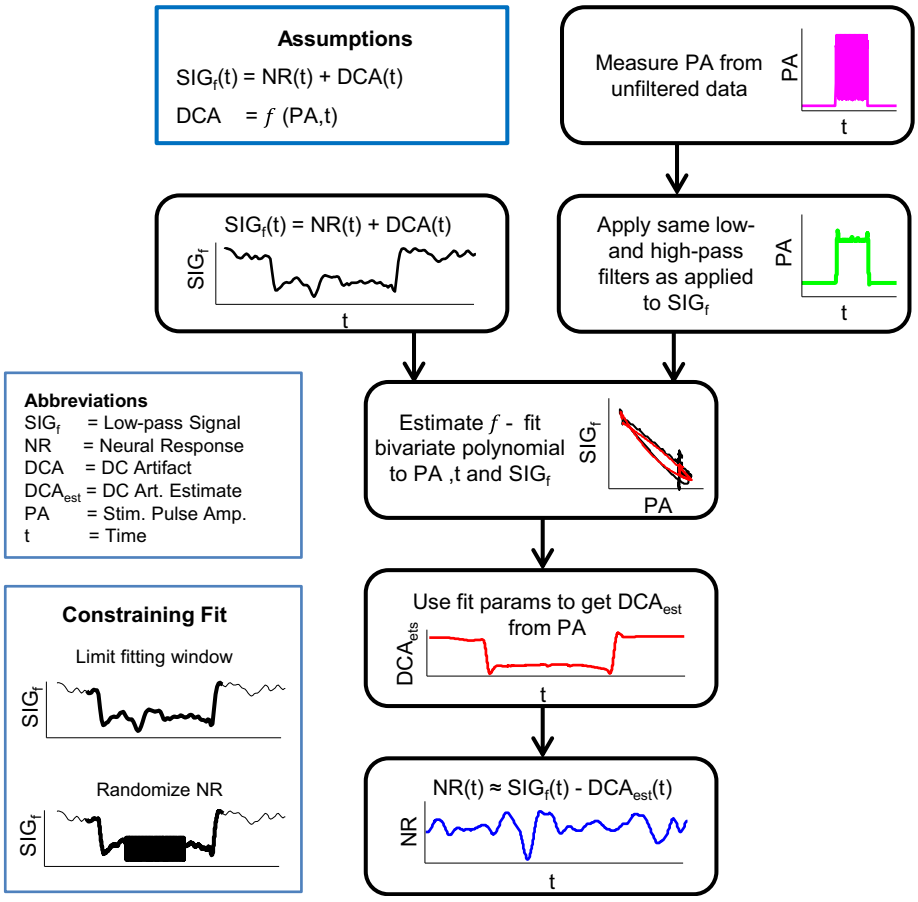

Fig. 5. Flow chart showing how the DC artifact can be estimated from the stimulation pulse amplitude (measurable with high sample rate acquisition systems) or stimulus envelope (for low sample rate systems). The estimate of the DC artifact is subtracted from the low-pass filtered signal to leave the neural response.

1) The PA (or SE) time series has a similar shape to the DCA. If we conceptualize the estimation procedure as transforming this PA time series into the DCA_{est}, then the degree of the polynomial determines how non-linear this transformation will be. A polynomial degree was selected that was high enough to characterize this transformation but low enough to limit any fitting to the neural response. 2) Only a limited time window of the epoch, where the DCA is expected to occur, was used in the fitting procedure (see Fig. 5 'Constraining Fit' inset). This time window was determined by the stimulus duration and the amplifier low-pass filter setting. If the amplifier low-pass filter was set to DC or 0.03 Hz, then the DCA was limited to the stimulus duration and only this portion of the epoch was used in the fitting procedure (thick line on upper plot in inset). A low-pass filter setting of 1 Hz caused the DCA to be smeared out in time, and here a time window from stimulus onset to epoch end was used in the fitting procedure. 3) Finally, during a time window when it was expected that the DCA would be flat, i.e. 30 ms after stimulus onset and 30 ms before stimulus offset, the order of elements in the SIG_f vector was randomized (see Fig. 5 'Constraining Fit' inset, lower plot). The randomization procedure preserves the main statistical properties of SIG_f during this time window (i.e. mean and standard deviation are unchanged) but removes temporal features of the NR, thus constraining the fitting procedure to the DCA component.

3. Results

3.1. Attenuation of high frequency artifact

All subjects tested showed a HFA. Fig. 2 shows an example of the HFA, which was generally in the mV range, and the low-pass filter procedure used to attenuate it. The high temporal resolution of the acquisition system allows us to see that the HFA was caused by the CI stimulation pulses (Fig. 2D). Averaging across repetitions caused a reduction in the HFA amplitude as the stimulation pulses in each repetition were not synchronized (Fig. 2B). The frequency spectrum of the averaged unfiltered signal (Fig. 2E) showed a strong component at that user's stimulation rate and its harmonics. The HFA could be completely attenuated for all subjects with a 35 Hz low-pass software filter (2nd order Butterworth, Fig. 2F). Fig. 2C shows an LAEP collected from a CI subject after the HFA had been attenuated by filtering. The typical N1–P2 complex is visible. To examine how effective a hardware filter was at attenuating the HFA, LAEPs were collected from 3 subjects using a 30 Hz low-pass hardware filter on the amplifier (12 dB per octave). These were compared with LAEPs collected from the same subjects, during the same session, with a 100 kHz low-pass hardware filter and then subsequently digitally filtered with a low-pass 2nd order Butterworth filter. The effects of attenuating the HFA using the hardware and software filters were found to be similar.

3.2. RF coil related artifact

There are two possible sources of high frequency artifact when recording LAEPs from CI subjects: the stimulation pulses or the RF coil transmission. The close resemblance of the temporal waveform of the HFA to that of the stimulation pulses suggests that, with this recording setup, the HFA is caused by the stimulation pulses and not the RF coil transmission. RF coil transmission is in the MHz range and so should be removed by the hardware filter on the amplifier. However, due to inadequate hardware filters, sub-harmonics or aliasing, it is possible that the RF coils causes an artifact. The standard electrode configuration used a recording electrode on the mastoid contralateral to the CI. Since both the RF coil and stimulation pulse artifacts will decrease in amplitude with distance from the CI, this configuration helps minimize any artifact. To further investigate the possibility of an RF related artifact, we collected data with a modified electrode configuration: the contralateral mastoid electrode was moved to the mastoid ipsilateral to the CI. Examination of the unfiltered data in both the temporal and spectral domains showed no evidence for a RF coil related artifact (see Supplementary Fig. 1 for a comparison of the amplitude spectra). The components present in data recorded with the standard electrode configuration were present in data recorded with an electrode on the ipsilateral mastoid.

To investigate this possibility that the DC artifact is caused by an RF coil related artifact and not the stimulation pulses, we collected data from one subject with a recording electrode on the ipsilateral mastoid, using stimuli with different shaped envelopes (Fig. 3A–F). Panels A, B and C show the unfiltered averaged data and panels D, E and F show the corresponding DC artifact after low-pass filtering. We know from CI encoding strategies (Zeng et al., 2008) that the stimulus envelope is directly related to the stimulation pulse amplitude, while in the RF transmission the amplitude of the stimulation pulses in not linearly encoded. Therefore, if the DC artifact is caused by the RF coil transmission its shape will be unaffected by the stimulus envelope. Fig. 3A–F shows that this is not the case: the shape of the DC artifact clearly follows the fluctuations in the pulse amplitude, indicating that the DC artifact is dominated by a component caused by the stimulation pulses. However, we cannot rule out the possibility that a small RF coil related component contributes to the DC artifact. Fig. 3G shows data from a different subject recorded with the standard electrode configuration at different stimulation levels. Plotting DC artifact amplitude against pulse amplitude shows a clear linear relationship. Since pulse amplitude is not linearly encoded in the RF transmission, any RF artifact would not decrease with decreasing pulse amplitude.

3.3. Attenuation of DC artifact

3.3.1. Attenuation by impedance balancing

After the HFA had been attenuated by low-pass filtering, the LAEPs for some subjects showed a DCA. Fig. 4A shows an example of a typical DCA, visible after low-pass filtering. In general, it was found that the size of the DCA was related to the size of the impedance mismatch between electrodes. Balancing electrode impedance reduced the size of the DCA and, in some cases, completely attenuated the DCA. For the LAEPs shown in Fig. 4A, where a large DCA is apparent, electrode impedances were Cz = 4.6 kΩ, Mastoid = 2.9 kΩ and Ground = 2.7 kΩ. Reducing the impedance on Cz to 2.6 kΩ completely attenuated the DCA (Fig. 4, blue line). Applying a low-pass filter to remove the HFA and ensuring that electrode impedances were balanced to within 1 kΩ produced LAEPs that contained no visible artifacts for 27% ($n = 6$) of subjects tested. Of the 6 subjects who showed no visible artifact after low-pass filtering, 4 used CIs from Cochlear, 1 was a Med-El user and 1 was an Advanced Bionics users. For the remaining 73% ($n = 16$), even after impedance balancing, a DCA artifact was present. This DCA was removed using the DCA estimation procedure, the results of which are reported in the following section.

To further examine the cause of the DCA, we selected 3 subjects who did not show a DCA. In these subjects, after the electrode impedances had been balanced, a DCA could be created by adding a 10 kΩ resistor between one of the electrode leads and the amplifier (Fig. 4B). After the resistor was removed the DCA was not present (Fig. 4D, blue line).

The cases where the DCA artifact was present and could be removed by impedance balancing or when the DCA was created by adding a resistor provided a useful method for validating the DCA estimation approach described below. The green lines in Fig. 4C and

D show the LAEPs obtained after applying the DCA estimation approach to the LAEPs shown in Fig. 4A and B, respectively. The blue and green lines in Fig. 4C and D show good agreement in shape and peak timing, indicating that the DCA artifact estimation approach attenuated the artifact just as effectively as the impedance balancing method.

3.3.2. Attenuation by DC artifact estimation

Fig. 6 shows an example of the different stages in the DCA estimation approach and compares the LAEPs obtained using the PA and SE methods. Fig. 6A shows the PA measured as the difference between the minimum and maximum values of each pulse in the unfiltered signal (purple line). The same band-pass filter used on the signal (high-pass from the amplifier and low-pass used in software to remove the HFA) was then applied to the PA. The purple and green lines in Fig. 6A show the PA before and after filtering, respectively. The black line in Fig. 6B shows the filtered signal (NR + DCA) plotted against the filtered PA. A 3rd degree bivariate polynomial was fitted to these data (i.e. PA, *t*, and NR + DCA). There was good agreement between the fitted polynomial function (Fig. 6B, red line) and the data (black line). The coefficients estimated from the fit were used in Eq. (3) to obtain an estimate of the DCA from the PA (Fig. 6E, red line). The blue line in Fig. 6E shows the NR, where the DCA has been attenuated by subtracting DCA_{est} (red line) from NR + DCA (black line). Supplementary Fig. 2 shows a three dimensional representation of the dataset before (NR + DCA) and after (NR) the attenuation of the DCA, where amplitude is coded as a color, repetitions are plotted on the *y* axis and time on the *x* axis. It is apparent that the DCA is present across different repetitions and that it is synchronized with stimulus onset and offset.

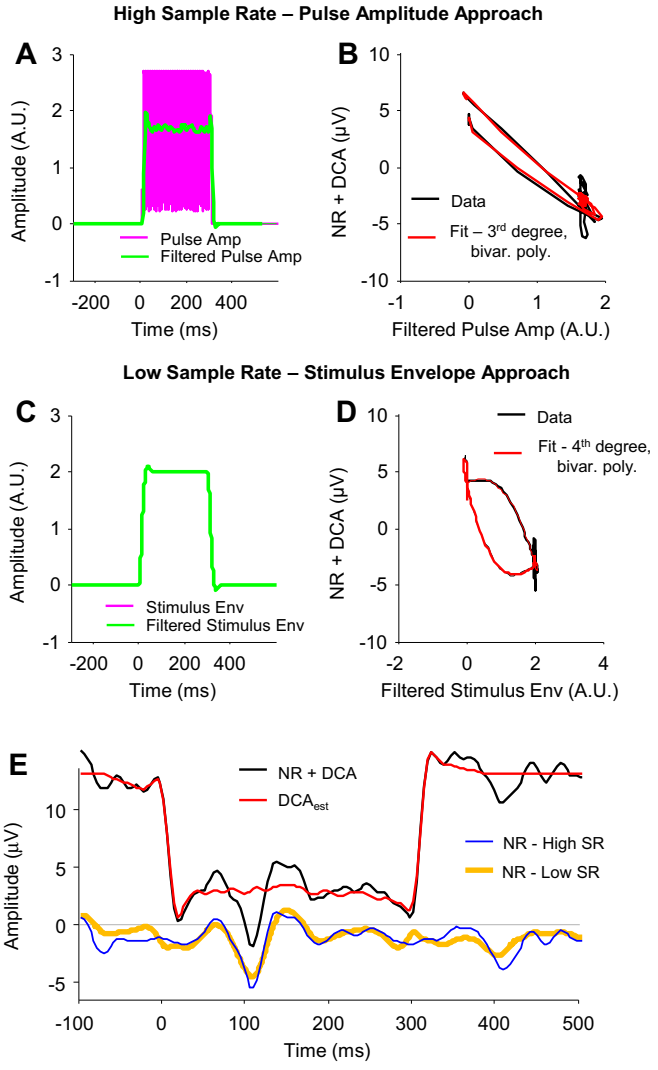

Fig. 6. DC artifact attenuation. A) Stimulation pulse amplitude as a function of time (purple line) was band-pass (0.03–35 Hz) filtered (green line) with the same filter applied to the signal. B) Plot of the low-pass filtered signal (NR + DCA) against pulse amplitude (Data, black line). The relationship was well described by a 3rd degree bivariate polynomial (Fit, red line). C) With lower sample rate data a measurement of stimulus envelope (purple line) is substituted for PA. The same filter that was applied to the signal was applied to the stimulus envelope measurement (green line). D) Plot of the low-pass filtered signal (NR + DCA) against stimulus envelope (Data, black line). The relationship was well described by a 4th degree bivariate polynomial. E) Subtracting DCA_{est} artifact (red line, estimated from PA. Stimulus envelope estimate not shown) from the low-pass filtered signal (NR + DCA, black line) leaves the NR. The blue line shows the NR obtained from the pulse amplitude approach and the orange line shows the NR obtained from the high stimulus envelope approach. (For interpretation of the references to colour in this figure legend, the reader is referred to the web version of this article.)

With most commercial acquisition systems it is not possible to acquire data at a sample rate high enough to resolve individual stimulation pulses, making it difficult to obtain the measurement of PA shown in Fig. 6A. To accommodate data acquired with low sample rate systems, we developed a method of estimating of the DCA using the stimulus envelope (SE). To directly compare the two methods, the data shown in Fig. 6 were downsampled to 1250 S/s, simulating data acquired with a commercial acquisition system. The SE was obtained by rectifying and low-pass filtering (35 Hz, 2nd order Butterworth) the stimulus. As with the PA, the same band-pass filter as applied to the signal was then applied to the SE. The green line in Fig. 6C shows the band-pass filtered SE, which in this case is almost identical to the SE (purple line, not visible) because the amplifier high-pass filter cutoff frequency was close to DC (0.03 Hz) and its effect was negligible. However, as shown in Fig. 7, when the cutoff frequency of the high-pass filter is further from DC its effects become more significant, making it important to include this step. The black line of Fig. 6D shows the downsampled filtered signal (NR + DCA) plotted against the SE. Here, the data (SE, *t*, and NR + DCA) were well fitted by a 4th degree bivariate polynomial (Fig. 6D, red line). In Eq. (3), PA was substituted by SE and the coefficients determined from the fit were used to obtain an estimate of DCA from SE and *t*. The NR, obtained by subtracting DCA_{est} from the downsampled NR + DCA, is shown as the yellow line in Fig. 6E (offset from zero). The high sample rate NR (blue line) compares well with the low sample rate NR (yellow line). The high sample rate method gave an N1–P1 amplitude of 4.9 μV while the low sample rate method gave an N1–P1 amplitude of 4.2 μV. The high and low sample rate N1 latencies were 109 and 107 ms, respectively.

The data shown in Figs. 6 and 7 were collected using 300 ms duration tonal stimuli with a non-fluctuating envelope. Therefore, the onset and offset of the DC artifact did not overlap in time with the N1 response and the DC artifact was flat during the N1 response. The method was tested using shorter duration stimuli (100 ms tones with a non-fluctuating envelope) where the DC artifact offset overlaps in time with the N1 response. Fig. 4B and D clearly show that the DC estimation procedure robustly attenuates the artifact even when neural response and stimulus offset overlap in time. This set of experiments did not test the DC artifact estimation procedure using stimuli with low frequency fluctuating envelopes. It is expected that the procedure would need to be adjusted to robustly attenuate DC artifacts which fluctuate during the neural response of interest.

3.3.3. DC artifact estimation – parameter study

A study was undertaken to evaluate the effect of different parameter settings on the DC artifact estimation procedure. The

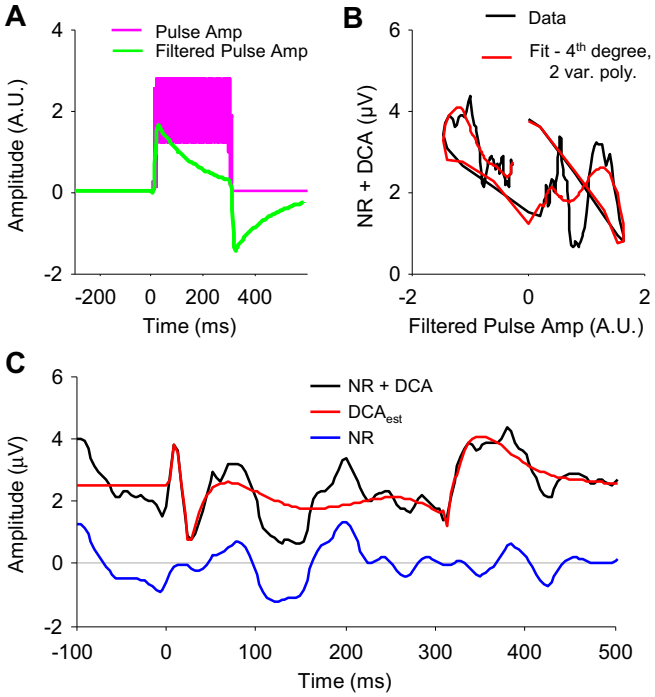

Fig. 7. Effect of the amplifier high-pass filter on the DC artifact. A) Stimulation pulse amplitude as a function of time (purple line) was band-pass (1–35 Hz) filtered (green line) with the same filter applied to the signal. B) Plot of the low-pass filtered signal against pulse amplitude (Data, black line). The relationship is best described by a 4th degree polynomial (Fit, red line). C) Subtracting DCA_{est} (red line) from the low-pass filtered signal (NR + DCA, black line) leaves the NR (blue line). (For interpretation of the references to colour in this figure legend, the reader is referred to the web version of this article.)

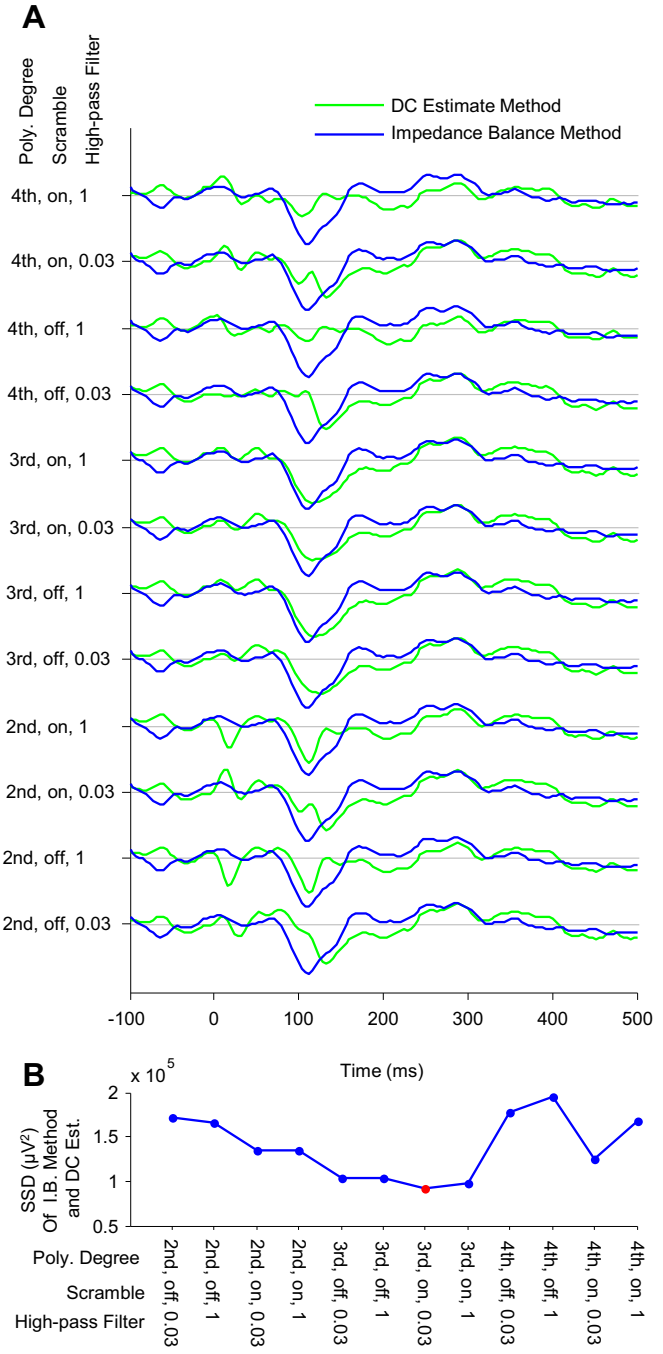

Fig. 8. Parameter study of DC artifact estimation procedure. A) The effect of changing polynomial degree, the scrambling procedure, and the filter applied to the PA, is shown for one LAEP (green lines, 12 parameter combinations). This is compared with an LAEP, collected from the same subject, where the artifact was attenuated using the impedance balancing method (blue lines, measured once). B) The sum of the squared differences (SSD) was calculated between the blue line and each of the lines for the different parameter combinations. (For interpretation of the references to colour in this figure legend, the reader is referred to the web version of this article.)

green lines in Fig. 8A show the effect of changing the degree of the polynomial from 2 to 4, the effect of the scrambling procedure (on or off), and the effect of including the amplifier high-pass filter setting (0.03 or 1 Hz). The effectiveness of the procedure was measured by calculating the sum of the squared differences (SSD) between the LAEP when the artifact was attenuated using the DC estimation procedure (green line, estimated for 12 parameter combinations) and the LAEP, measured using the same subject during the same recording session, when the artifact was attenuated using the impedance balancing procedure (blue line, measured once). Fig. 8B shows how this metric changes for different combinations of parameter settings. During this recording session the high-pass filter on the amplifier was set to 0.03 Hz. The parameter study shows that in this case the best artifact attenuation, using the DC estimation procedure, was achieved with a 3rd degree polynomial, applying the scrambling procedure, and filtering the PA with a high-pass setting that matched that used on the amplifier (i.e. 0.03).

In general, it was found that if the high-pass filter on the amplifier was set to DC or 0.03 Hz and the PA method was used, then the data (PA, *t* and NR + DCA) were well fitted by a 3rd degree polynomial. When the high-pass filter on the amplifier was set to DC or 0.03 Hz and the SE method was used, the data were best fitted with a 4th degree polynomial (Fig. 6C–E), the extra degree here accounting for the non-linear transformation between SE and PA. When the high-pass filter was set to 1 Hz, it produced a non-linear distortion of the DCA (Fig. 7C), i.e. the DCA became smeared out in time. Data acquired with these settings were best fitted by a 4th degree polynomial (Fig.7A and B).

3.4. Amplitude growth functions

The single-channel three stage artifact attenuation attenuated both the HFA and the DCA for all subjects tested. Out of the 22 subjects tested, 20 showed the typical N1–P2 complex in the LAEP. Two subjects did not show any significant peaks in the LAEP. To test the robustness of the approach, N1–P2 amplitude growth functions were collected for 6 of the 7 subjects tested at UC Irvine.

Fig. 9 shows the LAEP waveforms (blue lines) collected for one subject at MCL and at 7 other levels spaced in equal decibel steps down to threshold. N1 was defined as the minimum in the LAEP between 50 and 200 ms and P2 as the maximum occurring within 150 ms after N1. N1 and P2 are marked with blue circles in Fig. 9. To calculate a noise floor for each LAEP, the standard error for each time point in a long epoch (300 ms pre-stimulus to 800 ms post-stimulus) was calculated from the un-averaged, artifact attenuated, data. To do this the DCA calculated from the averaged data was subtracted from each un-averaged epoch. This noise estimation approach is similar to that used by Elberling and Don (1984) to estimate the noise in ABR recordings. It was observed that the standard error did not vary a lot as a function of time point, i.e. the standard error during time points with large neural response was similar to standard error during time points with no neural response. Therefore, the standard error was averaged across all time points within one recording to provide a single-number quantification of the noise in a recording. A noise floor (Fig. 9, gray lines) was defined at ±1.5 times the mean standard error, for the reason described below.

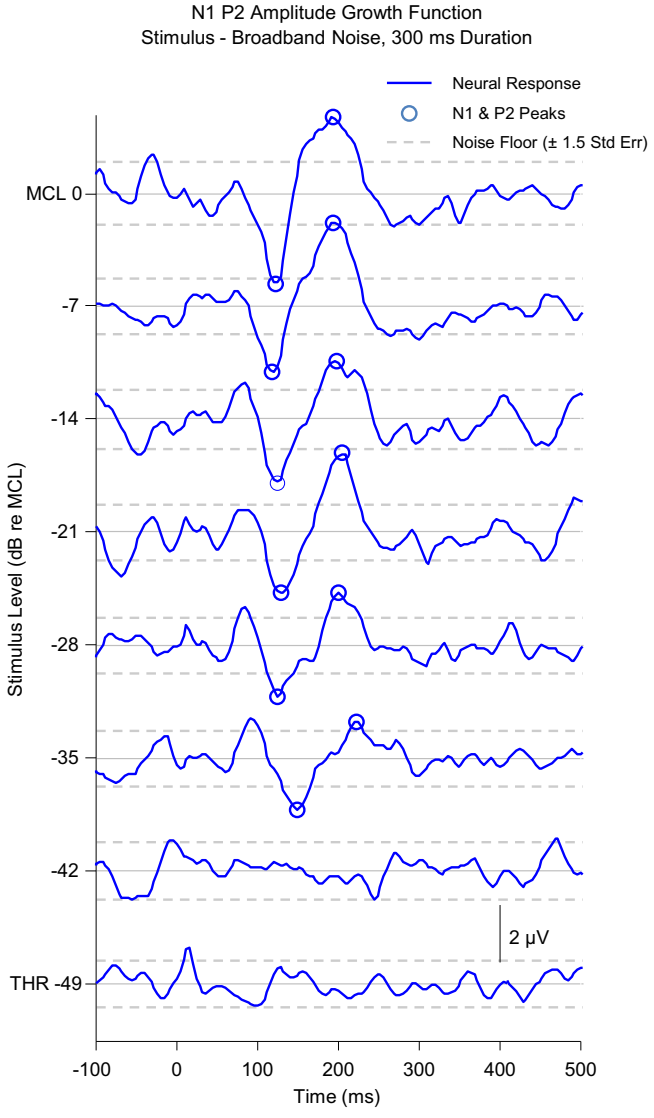

Fig. 9. LAEP amplitude growth function. LAEPs (blue lines) were obtained at 8 levels, equally spaced on a dB scale from most comfortable level (MCL) to threshold (THR). N1 and P2 peaks were extracted (open circles). The latency of the N1 peak was only considered significant if was above a noise floor (dashed gray line). (For interpretation of the references to colour in this figure legend, the reader is referred to the web version of this article.)

Figs. 10 and 11 show amplitude and latency metrics extracted from 11 N1–P2 amplitude growth functions measured from 10 different ears of 6 subjects. The stimuli were 300 ms duration tones with frequencies of 250, 500 or 1000 Hz. The difference in amplitude between the N1 and P2 peaks is shown as a function of stimulus level in Fig. 10. Some N1–P2 amplitude growth functions had a linear shape (e.g. Fig. 10F), while others showed a plateau above a certain level (e.g. Fig. 10A). The shape was not always consistent between ears of the same subject (compare Fig. 10B and C). Note that these amplitude growth functions were collected by stimulating through the subject's clinical processor and so they include the effects of the compression function used in the speech processing strategy. Fig. 11 shows the latency of the N1 peak, which either remained constant or showed an increase with decreasing level for all subjects. Only latencies where N1 amplitude was above the noise floor are shown. Taking the subject population as a whole, a value of 1.5 times the standard error was found to eliminate spurious N1 latency values at lower stimulation levels when the N1 amplitude became small. As a result of this criterion, there are often less points on Fig. 11 than on the corresponding panel on Fig. 10. For all 20 subjects, when stimulated at MCL, the mean N1–P2 amplitude was 5.4 (SD = 2.1) µV and the mean N1 latency was 111 (SD = 19) ms.

4. Discussion

We use the term artifact attenuation, rather than artifact removal or cancellation, as we cannot be certain that the artifact (HFA or DCA) was completely removed. Successful attenuation of artifact was judged by visual inspection of the LAEP. However, three points provide reassurance that, after the single channel artifact attenuation procedure has been applied, the effect of any remaining artifact on the neural response is negligible. Firstly, the impedance balancing procedure was used to validate the DCA estimation procedure. The LAEPs obtained using the DCA estimation procedure (Fig. 4C and D, green lines) shows good agreement with the LAEP obtained using the impedance balancing method. Secondly, N1–P2 amplitudes and N1 latencies obtained at MCL are comparable to those reported in other studies. Viola et al. (2011) used the multi-channel ICA approach to measure LAEPs for 18 CI subjects. They reported a mean N1–P2 amplitude of 8.9 (±4.1 standard deviation) µV and mean N1 latency of 132 (±13.7 standard deviation) ms. Finally, the amplitude growth functions (Figs. 9–11) show that N1–P2 amplitudes increase and N1 latencies decrease with increasing level, as has been previously reported for normal hearing subjects (for a summary, see Picton et al., 1976).

Below we give a list of recommendations for recording LAEPs for CI subjects and describe the best practice for applying the single channel approach. We discuss potential causes of the DCA. We then compare our single channel artifact attenuation approach with other approaches used to attenuate the HFA and DCA. Finally, we discuss the clinical use of LAEPs for assessing CI functionality and suggest how the single channel approach may facilitate their application.

4.1. Recording recommendations

As a first step to attenuating the DCA we recommend ensuring that all electrode impedances are balanced to within 1 kΩ. If the DCA persists, setting the high-pass filter on the amplifier to DC or 0.03 Hz will give the clearest acquisition of the DCA and allow the most straightforward application of the DCA estimation approach. When available (i.e. with high sample rate systems), we

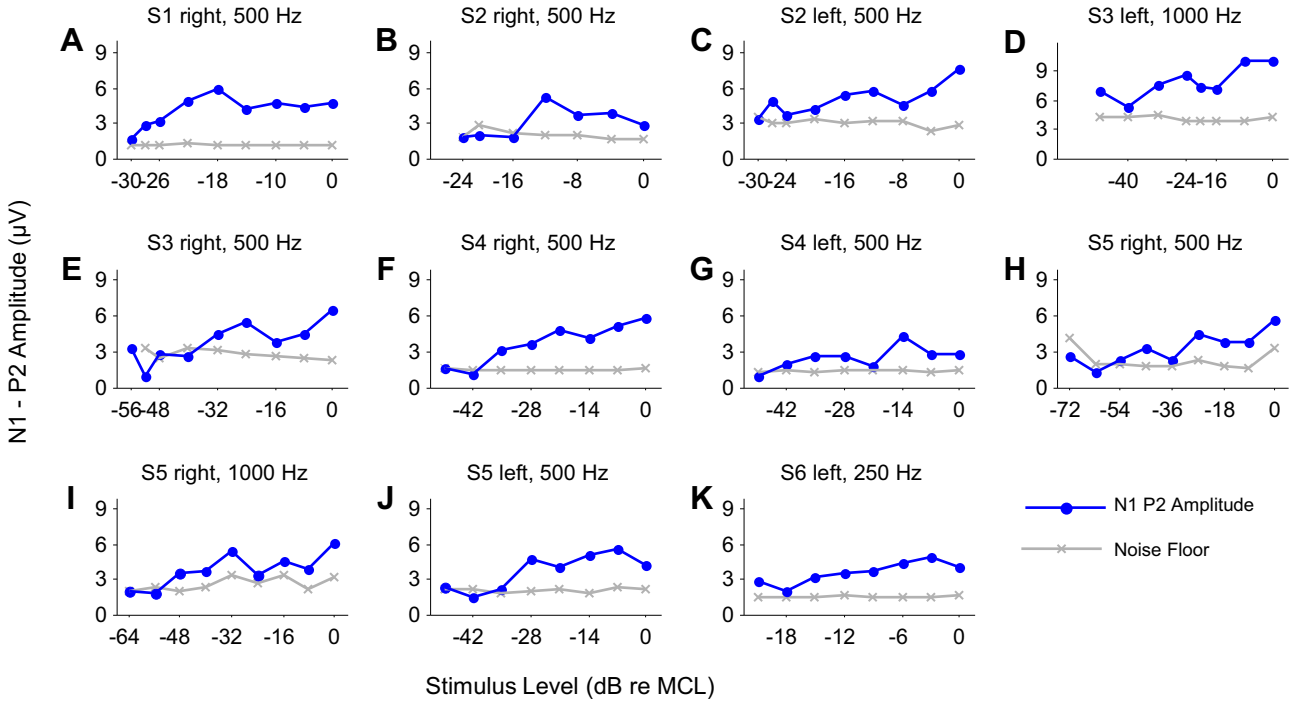

Fig. 10. N1–P2 amplitude growth functions for all subjects.

recommend using a measure of PA to estimate and then attenuate the DCA. When the amplifier high-pass filter is at DC or 0.03 Hz, the data (PA, *t* and NR + DCA) are best fitted with a 3rd degree bivariate polynomial. If a measure of PA is not available (low sample rate systems), a measure of SE can be substituted and the bivariate polynomial degree should be increased by one to account for the extra non-linear transformation between PA and SE. If the data were acquired with the amplifier high-pass filter at 1 Hz, the bivariate polynomial degree should be increased by 1 to account for the non-linear effects of the filter.

4.2. Potential causes of the DCA

With this recording system, the data show that the DCA is related to the stimulation pulse amplitude (Fig. 3) and that an electrode impedance mismatch can cause a DCA (Fig. 4). However,

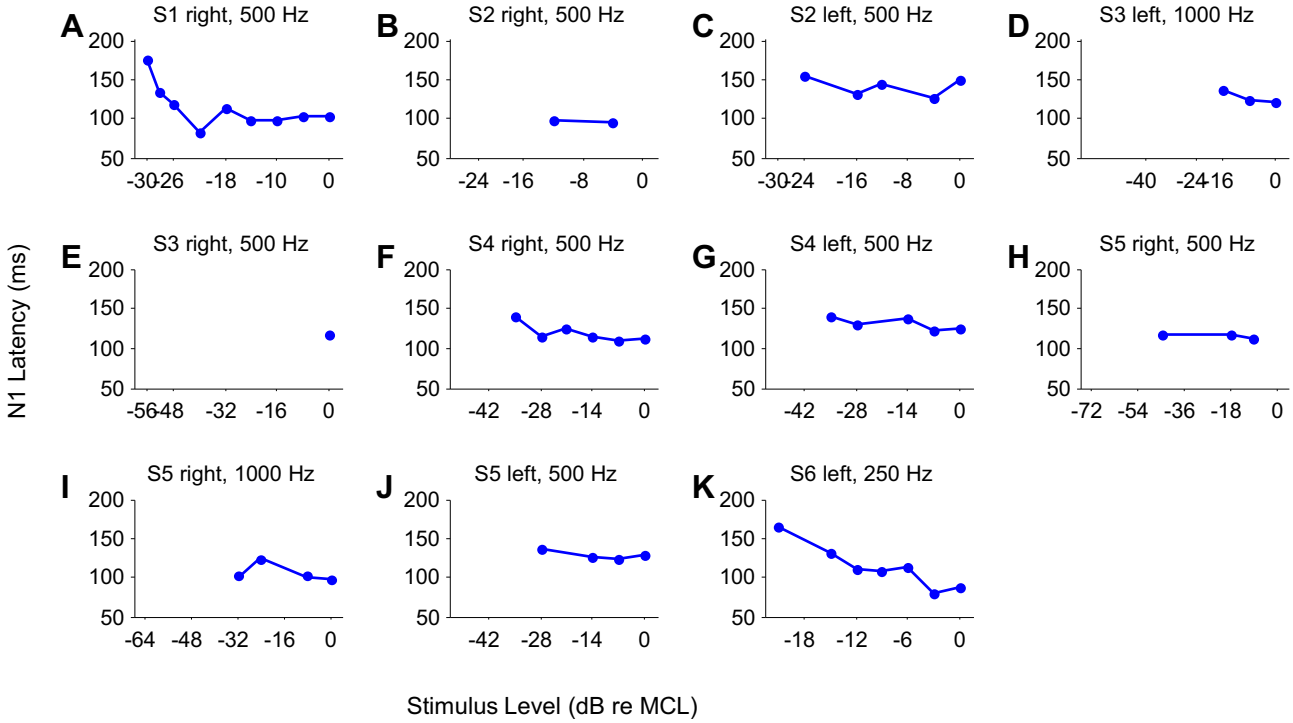

Fig. 11. N1 latency functions for all subjects.

we do not know the mechanism by which these factors cause or generate the DCA. It is possible that unwanted capacitance effects cause the DCA. These capacitances could be located at the CI electrode–neuron interface or at the EEG electrode–scalp interface. The stimulation pulse may deposit charge on this capacitor which is slowly released, causing the DCA. For some subjects ($n = 6$) the DCA can be removed by balancing the impedance of the scalp electrodes. For other subjects ($n = 16$), even when the scalp electrode impedances are balanced, the DCA is still present. For these subjects the DCA may be caused by an internal impedance path mismatch (i.e. from CI electrode to EEG scalp electrode). For normal hearing subjects a scalp electrode impedance mismatch may result in noisier recordings but it does not typically cause a DCA. Therefore, for CI subjects the DCA is likely caused by the large amplitude stimulation pulses in combination with an impedance mismatch or capacitance effect. Further experiments are necessary to test these hypotheses.

The auditory sustained potential is a low frequency, sustained, neural response with onset times of around 150 ms and amplitude to 6 μV (Picton et al., 1978). It is possible that this auditory sustained potential contributes to the low frequency component which we label as the DCA. Three pieces of evidence suggest that the DCA is dominated by artifact and not neural response: 1) The DCA has an onset time close to stimulus onset time while the sustained potential has a much later onset time. 2) The amplitude of the DCA can often be reduced by matching electrode impedance. 3) For some subjects, when electrode impedances are not matched, the amplitude of the DCA can be as large as 50 μV.

4.3. High frequency artifact attenuation

Most evoked potential studies using CI subjects use either a hardware or software low-pass filter with a cutoff frequency at around 50 or 35 Hz. The work presented here demonstrates that this low-pass filter will attenuate the HFA. Recent studies by Hofmann and Wouters (2010, 2012) used a high sample rate system to record auditory steady state responses from CI users. Their system could clearly resolve individual stimulation pulses, but rather than using a filtering approach, they showed that locating each stimulation pulse and linearly interpolating through it also removed the HFA. An interpolation approach to removing the HFA would also work with the system developed here. However, in practice filtering is easier to implement and more robust.

4.4. DC artifact estimation procedure

This study used tone or noise stimuli of 100, 300 or 500 ms duration where the temporal envelope contained only very fast fluctuations and the low frequency temporal envelope was non-fluctuating. This non-fluctuating, low frequency, stimulus envelope means that, just after stimulus onset and just before stimulus offset, the DC artifact will be flat. Since we know that the DC artifact will be flat in this period we can apply the randomization procedure described in Methods 2.4.3, *Constraining the Fit*. This will ensure that the fitting algorithm only fits to the mean amplitude (preserved by the randomization procedure) and not to any neural response (destroyed by the randomization procedure). To expand the DC estimation procedure to function with stimuli with a low frequency fluctuating envelope it would be necessary to remove the randomization procedure. This was not tested in this set of experiments and more work is needed to investigate the feasibility of using the DC estimation procedure with stimuli with fluctuating envelopes.

4.5. Clinical application of LAEP to CI users

A number of studies have indicated that cortical evoked potentials may be useful for predicting speech perception outcomes for CI subjects (Wable et al., 2000; Firszt et al., 2002; Kelly et al., 2005; Zhang et al., 2011), more so than earlier evoked potential responses such as auditory nerve electric compound action potentials (ECAPs) or auditory brainstem responses (Miller et al., 2008). However, two factors appear to have limited the clinical application of cortical evoked potentials for CI subjects. The first factor is the CI related artifact. The ICA based approach is useful in a research setting but, because of the necessity for multi-channel data, its practical application in a clinical setting is limited. This study provides a solution to this problem by showing how the CI related artifact can be attenuated using only single channel data, which are more easily obtained in a clinical setting. Recent work by our group, Mc Laughlin et al. (2012) and Beynon et al. (2008, 2012) has shown how LAEPs can be measured for CI subjects using the CI itself as a recording device, removing the need to attach scalp electrodes or have a dedicated LAEP acquisition system. Combining the LAEP CI recording technique with this single channel artifact cancellation approach would greatly increase the ease of access to LAEPs: just as an ECAP can be measured directly from the CI, so too could LAEPs. The second factor hindering the use of cortical evoked potentials in clinical use is that a stimulation paradigm or neural response that shows a strong correlation with speech perception in a large population of CI users has yet to be found. Firszt et al. (2002) showed, for a small population of CI users, a significant correlation between speech perception in quiet and a measure of mid-latency Na–Pa amplitude normalized for different stimulation levels. Zhang et al. (2011) found that a mismatch negativity measure could discriminate between good and bad performers on a speech perception task. By eliminating the need for multi-channel recordings, thereby reducing recording times, the single channel approach should facilitate the study of larger populations of CI subjects and may help in the development of an improved neural objective measure of CI performance. Behaviorally, it has been shown that more complex stimuli which probe the spectral discrimination of CI user can be used to provide a reasonable estimate of speech perception (Henry and Turner, 2003; Henry et al., 2005; Won et al., 2007). A preliminary study by our group has shown that combining this single channel artifact cancellation approach with a mismatch negativity paradigm using spectrally rippled stimuli can provide an objective neural estimate of a CI user's spectral discrimination (Mc Laughlin et al., 2013).

5. Conclusions

The single channel artifact cancellation approach described here can successfully attenuate both the high-frequency artifact produced by a cochlear implant and the DC artifact. The main advantage of this approach is that only single channel data are needed, simplifying the hardware and software requirements. The single channel approach should facilitate research into LAEPs recorded from CI users and could help develop a clinically applicable objective neural metric of CI performance.

Acknowledgments

We gratefully acknowledge the generosity of John D'Errico for contributing the polyfitn function to the Matlab File Exchange. We thank all the cochlear implant subjects who participated in the experiments. We also thank the two reviewers and the associate editor for their helpful comments and suggestions. This work was

partly supported by a Marie-Curie International Outgoing Fellowship (FP7 IOF 253047).

Appendix A. Supplementary data

Supplementary data related to this article can be found at http://dx.doi.org/10.1016/j.heares.2013.05.006.

References

Beynon, A., Luijten, B., 2012. Intracorporeal cortical telemetry (ICT): capturing EEG with a CI. In: 7th International Symposium on Objective Measures in Cochlear and Brainstem Implants. Amsterdam, p. 24.

Beynon, A., Luijten, B., Snik, A., 2008. The cochlear implant as an EEG-system: a feasibility study to measure evoked potentials beyond the ecap. In: 10th International Conference on Cochlear Implants and Other Implantable Auditory Technologies. San Diego.

Elberling, C., Don, M., 1984. Quality estimation of averaged auditory brainstem responses. Scand. Audiol. 13, 187–197.

Firszt, J.B., Chambers, R.D., Kraus, N., 2002. Neurophysiology of cochlear implant users II: comparison among speech perception, dynamic range, and physiological measures. Ear Hear. 23, 516–531.

Fu, Q.-J., 2002. Temporal processing and speech recognition in cochlear implant users. Neuroreport 13, 1635–1639.

Gilley, P.M., Sharma, A., Dorman, M., Finley, C.C., Panch, A.S., Martin, K., 2006. Minimization of cochlear implant stimulus artifact in cortical auditory evoked potentials. Clin. Neurophysiol. 117, 1772–1782.

Henry, B.A., Turner, C.W., 2003. The resolution of complex spectral patterns by cochlear implant and normal-hearing listeners. J. Acoust. Soc. Am. 113, 2861–2873.

Henry, B.A., Turner, C.W., Behrens, A., 2005. Spectral peak resolution and speech recognition in quiet: normal hearing, hearing impaired, and cochlear implant listeners. J. Acoust. Soc. Am. 118, 1111–1121.

Hofmann, M., Wouters, J., 2010. Electrically evoked auditory steady state responses in cochlear implant users. J. Assoc. Res. Otolaryngol. 11, 267–282.

Hofmann, M., Wouters, J., 2012. Improved electrically evoked auditory steady-state response thresholds in humans. J. Assoc. Res. Otolaryngol. 13, 573–589.

Kelly, A.S., Purdy, S.C., Thorne, P.R., 2005. Electrophysiological and speech perception measures of auditory processing in experienced adult cochlear implant users. Clin. Neurophysiol. 116, 1235–1246.

Mc Laughlin, M., Lopez Valdes, Alejandro, Viani, L., Walshe, P., Smith, J., Reilly, R.B., Zeng, F.-G., 2013. A spectrally rippled noise mismatch negativity paradigm for objectively assessing speech perception in cochlear implant users. In: 36th Annual Midwinter Meeting Abstract Book. Baltimore, p. 184.

Mc Laughlin, M., Lu, T., Dimitrijevic, A., Zeng, F.-G., 2012. Towards a closed-loop cochlear implant system: application of embedded monitoring of peripheral and central neural activity. IEEE Trans. Neural Syst. Rehabil. Eng. 20, 443–454.

Miller, C.A., Brown, C.J., Abbas, P.J., Chi, S.-L., 2008. The clinical application of potentials evoked from the peripheral auditory system. Hear. Res. 242, 184–197.

Picton, T.W., Woods, D.L., Baribeau-Braun, J., Healey, T.M., 1976. Evoked potential audiometry. J. Otolaryngol. 6, 90–119.

Picton, T.W., Woods, D.L., Proulx, G.B., 1978. Human auditory sustained potentials. I. The nature of the response. Electroencephalogr. Clin. Neurophysiol. 45, 186–197.

Viola, F.C., Thorne, J.D., Bleeck, S., Eyles, J., Debener, S., 2011. Uncovering auditory evoked potentials from cochlear implant users with independent component analysis. Psychophysiology 48, 1470–1480.

Wable, J., Van den Abbeele, T., Gallégo, S., Frachet, B., 2000. Mismatch negativity: a tool for the assessment of stimuli discrimination in cochlear implant subjects. Clin. Neurophysiol. 111, 743–751.

Won, J.H., Drennan, W.R., Rubinstein, J.T., 2007. Spectral-ripple resolution correlates with speech reception in noise in cochlear implant users. J. Assoc. Res. Otolaryngol. 8, 384–392.

Zeng, F.-G., Rebscher, S., Harrison, W.V., Sun, X., Feng, H., 2008. Cochlear implants: system design, integration and evaluation. IEEE Rev. Biomed. Eng. 1, 115–142.

Zhang, F., Anderson, J., Samy, R., Houston, L., 2010. The adaptive pattern of the late auditory evoked potential elicited by repeated stimuli in cochlear implant users. Int. J. Audiol. 49, 277–285.

Zhang, F., Hammer, T., Banks, H.-L., Benson, C., Xiang, J., Fu, Q.-J., 2011. Mismatch negativity and adaptation measures of the late auditory evoked potential in cochlear implant users. Hear. Res. 275, 17–29.